Ground state of a confined Yukawa plasma including correlation effects

C. Henning,[1] P. Ludwig,[1,2] A. Filinov,[1] A. Piel,[3] and M. Bonitz[1,*]
[1]*Institut für Theoretische Physik und Astrophysik, Christian-Albrechts-Universität zu Kiel, D-24118 Kiel, Germany*
[2]*Institut für Physik, Universität Rostock, Universitätsplatz 3, D-18051 Rostock, Germany*
[3]*Institut für Experimentelle und Angewandte Physik, Christian-Albrechts-Universität zu Kiel, D-24118 Kiel, Germany*
(Received 9 May 2007; published 14 September 2007)

The ground state of an externally confined one-component Yukawa plasma is derived analytically using the local density approximation (LDA). In particular, the radial density profile is computed. The results are compared with the recently obtained mean-field (MF) density profile [Henning *et al.*, Phys. Rev. E **74**, 056403 (2006)]. While the MF results are more accurate for weak screening, the LDA with correlations included yields the proper description for large screening. By comparison with first-principles simulations for three-dimensional spherical Yukawa crystals, we demonstrate that the two approximations complement each other. Together they accurately describe the density profile in the full range of screening parameters.

DOI: 10.1103/PhysRevE.76.036404 PACS number(s): 52.27.Jt, 52.27.Lw, 05.20.Jj, 52.27.Gr

I. INTRODUCTION

Interacting particles in confinement potentials are omnipresent in nature and laboratory systems such as trapped ions, e.g., [1,2], dusty plasmas, e.g., [3–5], or ultracold Bose and Fermi gases [6,7] and quantum confined semiconductor structures [8]. An interesting aspect of particle traps is that it is easy to realize situations of strong correlations. The observed particle arrangements extend from gaslike and liquidlike to solid behavior where the symmetry is influenced by the trap geometry. Of particular recent interest have been spherical traps, in which plasma crystals consisting of spherical shells (Yukawa balls) are formed, e.g., [9–11]. The particle distribution among the shells is by now well understood [11–13].

In a recent study [14], we also analyzed the average particle density in the trap and found that it is very sensitive to the binary interaction: it changes from a flat profile in the case of long-range Coulomb interaction to a profile rapidly decaying away from the trap center in the case of a screened Yukawa potential. Using a nonlocal mean-field (MF) approximation the density profile could be computed analytically and was found to agree very well with first-principles computer simulations for Yukawa crystals. However, when the screening is increased, deviations in the trap center kept growing, which was attributed to correlation effects missing in the mean-field model.

The goal of this paper is to remove these discrepancies. For this we extend the analysis of Ref. [14] by including correlation effects following an idea of Totsuji *et al.* [15] applied to two-dimensional systems. We apply the local density approximation (LDA) using known results [16] for the correlation energy of a homogeneous one-component Yukawa plasma. The results clearly confirm that correlation effects are responsible for the strong density increase in the trap center. We find that the LDA with correlations included agrees very well with simulations of Yukawa crystals in the limit of strong screening. On the other hand, for weak screening, the previous MF result turns out to be more accurate. Interestingly, for intermediate values of the screening parameter both methods are accurate, so a combination of both allows one to quantitatively describe the density profile in the whole range of screening parameters.

This paper is organized as follows. In Sec. II we introduce the LDA and use it first to compute the density profile in a mean-field approximation, which, of course, gives worse results than a MF calculation, but helps to understand the LDA. Then in Sec. III we improve the LDA model by including correlation effects. In Sec. IV the results for the density profile are compared to molecular dynamics simulations. A discussion is given in Sec. V.

II. GROUND STATE OF A CONFINED PLASMA WITHIN THE LDA

We consider N identical particles with mass m and charge Q confined by an external potential Φ and interacting with the isotropic Yukawa-type pair potential $V(r)=(Q^2/r)\times\exp(-\kappa r)$. To derive the properties of interest we start with the expression of the ground-state energy, which is given by

$$E[n]=\int d^3r\, u(\mathbf{r}), \tag{1}$$

with the energy density $u(\mathbf{r})=u^{\mathrm{conf}}(\mathbf{r})+u^{\mathrm{MF}}(\mathbf{r})+u^{\mathrm{cor}}(\mathbf{r})$, where the energy densities from confinement and from the mean-field interaction are

$$u^{\mathrm{conf}}(\mathbf{r})=n(\mathbf{r})\Phi(\mathbf{r}), \tag{2a}$$

$$u^{\mathrm{MF}}(\mathbf{r})=n(\mathbf{r})\frac{N-1}{2N}\int d^3r_2 n(\mathbf{r}_2)V(|\mathbf{r}-\mathbf{r}_2|). \tag{2b}$$

The correlation contribution u^{cor} will be discussed below (Sec. III) by means of the local density approximation. First, we introduce this approximation and obtain first the LDA results in the mean-field approximation (LDA-MF). These results will not be as accurate as the MF results, due to the applied approximation, but the LDA-MF helps in familiarization with the LDA and its characteristics.

*bonitz@physik.uni-kiel.de

The local density approximation is based upon the idea of replacing the nonlocal terms within the energy density at point $\mathbf{r}$ by local expressions using the known energy density of the homogeneous system with its density n_0 equal to the local density $n(\mathbf{r})$ of the true inhomogeneous system in question. Therefore, to derive the LDA-MF we need to substitute for the nonlocal term (2b), i.e., for the density of interaction energy, the corresponding expression of the infinite homogeneous system, which is given by (details are given in the Appendix)

$$u_0(\kappa) = n_0 \frac{N-1}{2N} Q^2 \int d^3 r_2 n_0 \frac{e^{-\kappa|\mathbf{r}-\mathbf{r}_2|}}{|\mathbf{r}-\mathbf{r}_2|} = \frac{N-1}{N} Q^2 n_0^2 \frac{2\pi}{\kappa^2}, \tag{3}$$

and, as a second step, replace the homogeneous density n_0 by the local density $n(\mathbf{r})$. Thus we obtain the LDA-MF ground-state energy

$$E_{\mathrm{LDA}}^{\mathrm{MF}}[n] = \int d^3 r\, u(\mathbf{r}) \tag{4}$$

with the energy density

$$u(\mathbf{r}) = n(\mathbf{r}) \left(\Phi(\mathbf{r}) + \frac{N-1}{N} Q^2 n(\mathbf{r}) \frac{2\pi}{\kappa^2} \right). \tag{5}$$

The variation of the energy

$$\tilde{E}_{\mathrm{LDA}}^{\mathrm{MF}}[n,\mu] = E_{\mathrm{LDA}}^{\mathrm{MF}}[n] + \mu \left(N - \int d^3 r\, n(\mathbf{r}) \right) \tag{6}$$

with respect to the density $n(\mathbf{r})$ (for details see Ref. [14]) yields an explicit expression for the density profile in an arbitrary confinement potential,

$$n(\mathbf{r}) = \frac{N\kappa^2}{4\pi(N-1)Q^2} [\mu - \Phi(\mathbf{r})], \tag{7}$$

which holds at any point where the density is positive. Due to (6) this density is normalized by

$$\int d^3 r\, n(\mathbf{r}) = N. \tag{8}$$

The case of isotropic confinement $\Phi(\mathbf{r}) = \Phi(r)$, which is of particular interest, leads to an isotropic density distribution $n(\mathbf{r}) = n(r) = \tilde{n}(r)\Theta(R-r)$, the outer radius R of which is fixed by the normalization condition (8), which now becomes $\int_0^R dr\, r^2 \tilde{n}(r) = N/4\pi$. In this isotropic case the yet unknown Lagrange multiplier μ can be obtained by taking the variation also with respect to R [15], which yields

$$\mu = \Phi(R). \tag{9}$$

Compared to the MF result, which was given in [14],

$$n^{\mathrm{MF}}(\mathbf{r}) = \frac{N}{4\pi(N-1)Q^2} [\Delta\Phi(\mathbf{r}) + \kappa^2 \mu^{\mathrm{MF}} - \kappa^2 \Phi(\mathbf{r})], \tag{10}$$

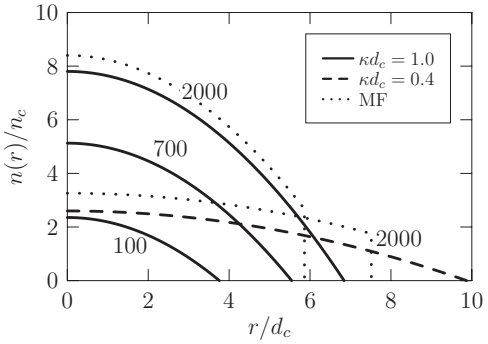

FIG. 1. Radial density profile for a parabolic confinement potential $\Phi(r) = (\alpha/2)r^2$, a constant screening parameter $\kappa d_c = 1$, and three different particle numbers $N = 100$, 700, 2000. The result for $\kappa d_c = 0.4$, $N = 2000$ is also shown by the dashed line. For comparison, the nonlocal MF results for $\kappa d_c = 0.4, 1.0$, $N = 2000$ are given by the dotted lines.

$$\mu^{\mathrm{MF}} = \Phi(R^{\mathrm{MF}}) + \frac{R^{\mathrm{MF}} \Phi'(R^{\mathrm{MF}})}{1 + \kappa R^{\mathrm{MF}}}, \tag{11}$$

the LDA-MF density (7) shows important differences. On the one hand, the Laplacian of the potential $\Delta\Phi(\mathbf{r})$ is missing and, on the other hand, the expression for the chemical potential μ is simpler than μ^{MF}. That is based upon the fact that the missing terms contain derivatives and thus information about contiguous values of the potential, which is suppressed within the LDA-MF and generally within the LDA. Consequently, the finite density jump at $r = R$, which is familiar from electrostatics of charged bodies and appears in the MF approximation, Fig. 1, is not reproduced by the LDA-MF.

A. Parabolic confinement potential

For the case of a parabolic external potential $\Phi(r) = (\alpha/2)r^2$ the density following from Eqs. (7) and (9) is

$$n(r) = \frac{\alpha N}{4\pi(N-1)Q^2} \left(\frac{\kappa^2 R^2}{2} - \frac{\kappa^2 r^2}{2} \right) \Theta(R-r). \tag{12}$$

The dimensionless combination κR, which contains the limiting outer radius, can be obtained from the normalization (8) and is given by

$$\kappa R = \sqrt[5]{\frac{15(N-1)Q^2\kappa^3}{\alpha}} = \sqrt[5]{\frac{15}{2}(\kappa d_c)^3 (N-1)}. \tag{13}$$

Here, we introduced the length scale $d_c = (2Q^2/\alpha)^{1/3}$, which is the stable distance between two charged particles in the absence of screening [11] and which will be used below as the proper unit for lengths and screening parameters. As the unit for densities we use the average density of a large Coulomb system, which is given by $n_c = (3\alpha)/(4\pi Q^2)$.

The results of (12) are shown in Fig. 1 for three particle numbers from $N = 100$ to 2000. One clearly sees the parabolic decrease of the density away from the trap center until it terminates in zero. The curvature of the density does not

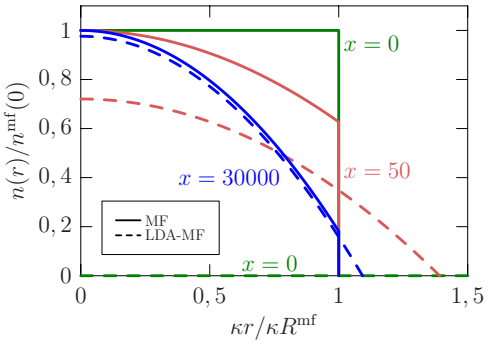

FIG. 2. (Color online) Radial MF density profile (solid lines) compared to the LDA-MF (dashed lines) for three different density parameters $x=(\kappa d_c)^3(N-1)$. The abscissa is normalized with the MF radius R^{MF}, while the ordinate is normalized with the corresponding MF density $n^{\mathrm{MF}}(0)$ at the trap center.

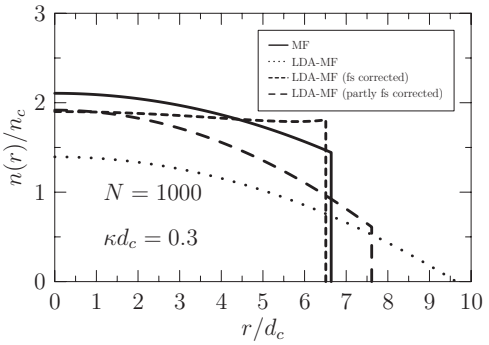

FIG. 3. Radial density profiles of a spherical plasma of $N=1000$ and $\kappa d_c=0.3$ calculated by the LDA-MF with (fs corrected) and without finite-size effects included. For comparison, the exact MF result is also given (solid line). The difference between the finite-size correction and the partial finite-size correction is described in the text.

change on increasing the particle number—just the density increases continuously at every space point and, at the same time, extends to higher values of the limiting radius R. However, the curvature of the density profile changes dramatically when the plasma screening is increased at constant N.

Thus, in the case of an isotropic parabolic potential, the LDA density profile bears a qualitative resemblance to the density profile in the nonlocal mean-field approximation, although in the case of other confinement potentials the deviations of the LDA-MF from the MF approximation are stronger [cf. Eqs. (7) and (10)]. However, quantitatively at two points the MF result differs from the LDA-MF for parabolic confinement as well, as can also be seen in Fig. 1.

First, the density in this local density approximation does not show a discontinuity at $r=R$, in contrast to the MF result, Eqs. (10) and (11). This is due to the neglect of edge effects in this derivation of the LDA result. Second, the LDA-MF yields too small values of the density. This error is reduced (see Fig. 2) with increasing values of the density parameter $x=(\kappa d_c)^3(N-1)$ (cf. Ref. [14]), which, regardless of the factor $N/(N-1)$, solely determines the density profile. The reason for this improved behavior with increasing x is that an increase of κ contracts the effective area of integration within (2b) as well as within (3). The contraction finally is in favor of the accuracy of the LDA-MF, because the decreased integration volume contains a more homogeneous density. Also, an increase of the particle number N, which flattens the density profile, will similarly improve the LDA-MF.

Because the validity of the mean-field model depends on the value of the screening parameter κd_c, there are the following two cases. In the first case, for small values of the screening parameter, the MF approximation provides a good description of the density profile, but the LDA-MF underrates this profile and so does not give a good description on its own. (That applies also if finite-size effects are included; see Fig. 3.) In the second case, for large values of the screening parameter, the LDA-MF approaches the MF approximation; however, there, the latter does not describe the density profile correctly due to the neglect of the now relevant correlation contributions [15]. Thus, the local density approximation of the mean-field energy alone does not give a good description of the density profile.

However, it gives a straightforward way to include the missing correlation contributions in the energy density by usage of the result for the homogeneous system; see Sec. III.

B. Improvement of the LDA by inclusion of finite-size effects

As can be seen from Fig. 2 and from Eq. (7) the density profile obtained by the LDA-MF breaks down in the Coulomb case—the density can no longer be normalized, which is the same as in the two-dimensional case [15]. But the application of a local density approximation cannot be the reason for this, because the method of the LDA is based upon the usage of results from the homogeneous system, and the Coulomb system is homogeneous with $n_0=[N/(N-1)]n_c$.

In fact, the cause of the breakdown is the use of results from the infinite homogeneous system, neglecting finite-size effects. This failure can be avoided by replacing (3) by the corresponding expression for the finite homogeneous system. In the Appendix such an expression is derived for isotropic confinement. As a result, the finite-size effects lead to a corrected density profile

$$n(r)=\frac{N\kappa^2}{4\pi(N-1)Q^2}\frac{\mu-\Phi(r)}{1-e^{-\kappa R}(1+\kappa R)\sinh(\kappa r)/(\kappa r)}\times\Theta(R-r), \tag{14}$$

instead of Eq. (7), which indeed yields the constant MF solution in Coulomb case also for the LDA-MF. As another example, in Fig. 3 the density profiles with [LDA-MF (fs corrected)] and without these finite-size contributions are shown for $N=1000$, $\kappa d_c=0.3$. One clearly sees that in the case of finite-size correction the density profile shows a discontinuity at the boundary and, due to that, it yields increased values of the density. However, the density profile including edge effects is not monotonically decreasing away from the trap center but has a density-increasing part in the outer range, which is not correct. This is due to the space dependence of the denominator of Eq. (14).

By contrast a more accurate monotonically decreasing density profile can also be obtained by taking the finite-size effects only partly into account [LDA-MF (partly fs corrected)], as derived in the Appendix. The final result is given by

$$n(r) = \frac{N\kappa^2}{4\pi(N-1)Q^2} \frac{\mu - \Phi(r)}{1 - e^{-\kappa R}(1+\kappa R)} \Theta(R-r), \quad (15)$$

which now misses the r dependence in the denominator. The corresponding result is also given in Fig. 3.

Consequently, for Yukawa systems like those analyzed here, an improvement of LDA is possible by including edge effects. However, for small values of the screening parameter even the improved local density approximation does not approach the degree of accuracy obtained by the nonlocal mean-field model MF (cf. Fig. 3). On the other hand, for increased screening the finite-size effects do not alter the density profile significantly.

Therefore, below we continue to use Eq. (3) from the infinite homogeneous system.

III. INCLUSION OF CORRELATION CONTRIBUTIONS

The energy expression $E_{\mathrm{LDA}}^{\mathrm{MF}}$ (4), (5) contains only the energy density of the confinement and of the mean-field interaction. To include the contribution of the particle correlations, we can make use of the result for the density of the correlation energy of the homogeneous system which is given by Eq. (3) of Ref. [16]:

$$u^{\mathrm{cor}}(n_0,\kappa) = -1.444Q^2 n_0^{4/3} \exp[-0.375\kappa n_0^{-1/3} + 7.4\times 10^{-5}(\kappa n_0^{-1/3})^4], \quad (16)$$

where n_0 is the corresponding density of the homogeneous system. By replacing this density with the local density $n(\mathbf{r})$ of the inhomogeneous system, one obtains the correlation contribution of the energy density within the LDA. Thus we derive the complete ground-state energy in the local density approximation,

$$E_{\mathrm{LDA}}[n] = \int d^3r\, u(\mathbf{r}), \quad (17)$$

with energy density

$$u(\mathbf{r}) = n(\mathbf{r})\Phi(\mathbf{r}) + \frac{N-1}{N} Q^2 n(\mathbf{r})^2 \frac{2\pi}{\kappa^2} - 1.444Q^2 n(\mathbf{r})^{4/3} \times \exp\{-0.375\kappa n(\mathbf{r})^{-1/3} + 7.4\times 10^{-5}[\kappa n(\mathbf{r})^{-1/3}]^4\}. \quad (18)$$

As before, variation of the energy (17) at constant particle number [cf. Eq. (6)] yields the ground-state density profile, but now with correlation effects included. In this case the strong nonlinear character of the energy density does not allow for an explicit solution. Just an implicit solution is possible and is given by the following equation for $z^3(\mathbf{r}) = \kappa^{-3} n(\mathbf{r})$, which can be regarded as the local plasma parameter of the system:

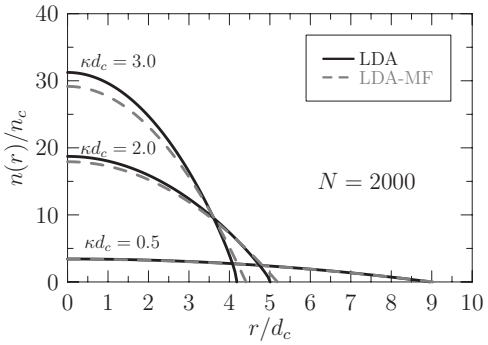

FIG. 4. Radial density profile of a confined spherical plasma of $N=2000$ particles calculated with the LDA including correlation contributions (solid lines) compared to the LDA-MF (dashed lines) for three different screening parameters.

$$0 = \frac{N-1}{N} z^3(\mathbf{r}) + \frac{\Phi(\mathbf{r}) - \mu}{4\pi Q^2 \kappa} - [c_1 z(\mathbf{r}) + c_2 - c_3 z(\mathbf{r})^{-3}] \times \exp[-0.375 z(\mathbf{r})^{-1} + 7.4\times 10^{-5} z(\mathbf{r})^{-4}]. \quad (19)$$

The constants c_i are given by

$$c_1 = 0.153, \quad (20a)$$

$$c_2 = 0.0144, \quad (20b)$$

$$c_3 = 1.134\times 10^{-5}. \quad (20c)$$

The solution of Eq. (19) can be obtained numerically. For the case of a parabolic external potential $\Phi(r)=(\alpha/2)r^2$ results are given in Fig. 4. There, the density profile of a plasma of $N=2000$ particles within LDA is shown for three different screening parameters: $\kappa d_c=0.5$, 2.0, and 3.0. For comparison the LDA-MF density profile is shown, too.

It can be seen that for a small screening parameter (see the line $\kappa d_c=0.5$) both density profiles are nearly identical. But with increasing screening, i.e., for smaller values of the local plasma parameter z^3, the correlation contributions within the LDA alter the curvature of the profile, which rises more steeply toward the center. So the particle correlations tend to increase the central density of the plasma, which can also be seen in Fig. 6 in comparison with the mean-field approximation.

IV. COMPARISON WITH SIMULATION RESULTS FOR FINITE YUKAWA CRYSTALS

We performed molecular dynamics simulations of the ground state of a large number of Coulomb balls for the purpose of comparison of their average density with the analytical results of the present model (for simulation details, see Refs. [10,11]). In order to obtain a smooth average radial density profile, the averaging process was accomplished by substituting for each particle a small but finite sphere. In Fig. 5 these smoothed density profiles are shown for different sphere radii of the particles: $0.3d_c$, $0.4d_c$, and $0.5d_c$. Also the average particle densities in the vicinity of the corresponding shells are shown (crosses). Note that there is only a small

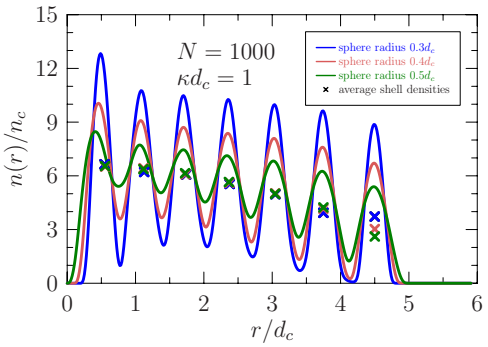

FIG. 5. (Color online) Smoothed density of a simulated spherical Yukawa crystal with $N=1000$ and $\kappa d_c=1$ with application of different sphere sizes for substitution of the particles: $0.3d_c$ (top curve), $0.4d_c$ and $0.5d_c$. The symbols show the averaged densities of the shells placed on the centers of mass of the shells.

range of reasonable sphere radii: for values smaller than $0.3d_c$ the shells break up into subshells, whereas for values larger than $0.5d_c$ the amplitude of the oscillations decreases further without effect on the average density. Only the outer shell density is somewhat sensitive to the sphere radius due to the increase of the size of this shell with increasing sphere radius. Therefore, for the comparisons below, we use the sphere radius corresponding to the average of the possible density values which, in the figure, is close to the value for $0.4d_c$.

Numerical results of the comparison with a Coulomb ball of $N=1000$ particles are included in Fig. 6 for four different screening parameters. The symbols denote the average shell density, while the lines represent the MF (solid) and the LDA density (dashed). For small values of the screening parameter $\kappa d_c<2$ the simulation results are very well reproduced by the analytical density profile of the nonlocal mean-field model (MF), whereas the local density approximation underrates the results [lower lines in Fig. 6(a)]. On the other hand, for larger values of the screening parameter $\kappa d_c>2$ the simulation results are reproduced by the LDA, whereas MF underestimates these results in the center. This underestimation is accompanied by a wrong prediction of the profile curvature [Fig. 6(b)]. For intermediate values of the screening parameter $\kappa d_c\approx 2$, both methods are very close to the averaged simulation results [upper lines in Fig. 6(a)]. We have verified this behavior also for other Coulomb balls. Another representative example is shown in Fig. 7 for a Coulomb ball with $N=10\,000$. There, the same behavior as in Fig. 6 is seen.

V. SUMMARY AND DISCUSSION

A theoretical analysis of the ground-state density profile of a spatially confined one-component plasma within the local density approximation was presented. We derived a closed equation, Eq. (19), for the density profile, including correlation effects for arbitrary confinement potentials with any symmetry. In contrast to the result without particle correlations, the density profile shows an increased central density with increasing screening parameter. The validity of the

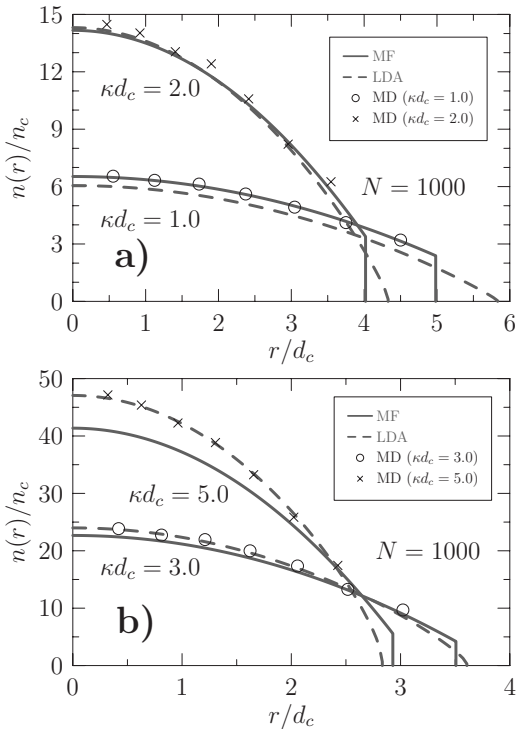

FIG. 6. Radial density profiles of a three-dimensional plasma of $N=1000$ particles calculated with the exact mean-field model (solid lines) and with the LDA including correlation contributions (dashed lines) for four different screening parameters: $\kappa d_c=1$, 2, 3, and 5. Averaged shell densities of molecular dynamics results of a plasma crystal for the same parameters are shown by the symbols. For details, see the discussion in Sec. IV.

LDA is, however, limited to not too small values of the screening parameter, $\kappa d_c\geq 2$.

Comparisons with first-principles simulation results of strongly correlated Coulomb clusters with varying screening parameter showed that the LDA allows one to remove the problem of the MF approximation observed in Ref. [14] which arises with increasing screening parameter. Therefore,

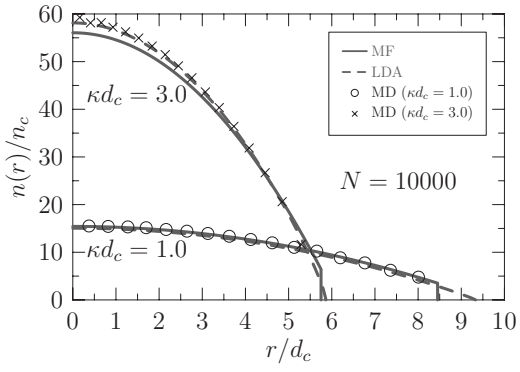

FIG. 7. Radial density profiles of a three-dimensional plasma with $N=10\,000$ and two different screening parameters ($\kappa d_c=1$, $\kappa d_c=3$). The solid (dashed) lines show MF (LDA) calculation results. Symbols denote molecular dynamics results of a plasma crystal for the same parameters where the average density at the positions of the shells is shown.

the mean-field model together with the presented local density approximation complement one another in the description of strongly correlated spatially confined one-component plasmas.

ACKNOWLEDGMENTS

The authors are indebted to D. Block and A. Melzer for fruitful discussions. This work is supported by the Deutsche Forschungsgemeinschaft via SFB-TR 24 Projects No. A3, No. A5, and No. A7.

APPENDIX: LOCAL DENSITY APPROXIMATION USING A FINITE REFERENCE SYSTEM

The investigation of an inhomogeneous system within the LDA uses known results from the corresponding homogeneous system. There, the infinite homogeneous system is often used as a reference system, which entails the neglect of finite-size effects. To take these into account, the finite homogeneous system has to be used as reference. In the present derivation such a modification is made for an isotropic confinement and leads to a change of the expression for the density of interaction energy, Eq. (3),

$$\begin{aligned} u_0(\kappa) &= n_0 \frac{N-1}{2N} Q^2 \int d^3 r_2 n_0 \frac{e^{-\kappa|\mathbf{r}-\mathbf{r}_2|}}{|\mathbf{r}-\mathbf{r}_2|} \\ &= n_0^2 \frac{N-1}{2N} Q^2 \int dr_2\, 4\pi r_2^2 \frac{e^{-\kappa r_2}}{r_2} \\ &= \frac{N-1}{N} Q^2 n_0^2 \frac{2\pi}{\kappa^2}. \end{aligned} \tag{A1}$$

This formula has no spatial dependence due to the infinite integration volume and it diverges in the limit of Coulomb interaction ($\kappa \to 0$), leading to a breakdown of the approximation.

By contrast, the density of interaction energy of the corresponding finite homogeneous system (a sphere with center $\mathbf{r}_2 = \mathbf{0}$ and radius R) is given by

$$\begin{aligned} u_0(\kappa, r) &= n_0 \frac{N-1}{2N} Q^2 \int_{\mathcal{S}(0,R)} d^3 r_2 n_0 \frac{e^{-\kappa|\mathbf{r}-\mathbf{r}_2|}}{|\mathbf{r}-\mathbf{r}_2|} \\ &= n_0^2 \frac{N-1}{2N} Q^2 \frac{2\pi}{\kappa r} \int_0^R dr_2 r_2 (-e^{-\kappa(r+r_2)} + e^{-\kappa|r-r_2|}) \\ &= n_0^2 \frac{N-1}{2N} Q^2 \frac{4\pi}{\kappa r} \left(e^{-\kappa r} \int_0^r dr_2 r_2 \sinh(\kappa r_2) \right. \\ &\quad \left. + \sinh(\kappa r) \int_r^R dr_2\, r_2 e^{-\kappa r_2} \right) \\ &= \frac{N-1}{N} Q^2 n_0^2 \frac{2\pi}{\kappa^2} \left(1 - e^{-\kappa R}(1+\kappa R) \frac{\sinh(\kappa r)}{\kappa r} \right), \end{aligned} \tag{A2}$$

including a finite-size contribution, which prevents the problem of divergence at $\kappa \to 0$. As already mentioned in Sec. II B the resulting density profiles show the incorrect behavior of a nonmonotonic density profile (cf. Fig. 3).

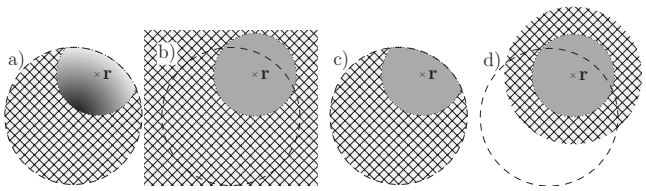

FIG. 8. Comparison of the MF method and the different LDA methods for calculating the energy density of interaction $u^{\mathrm{MF}}(\mathbf{r})$ in the case of finite screening: (a) MF, (b) LDA (infinite reference system), (c) LDA (fs corrected), and (d) LDA (partly fs corrected). Within the graphics the system is represented by the dashed line. The hatched region shows the integration area used within the method, whereas the solid gray region shows the effective integration area due to finite screening. The color gradient within (a) represents the nonconstant density of the system, which is taken into account within the MF method in contrast to the LDA methods, which take the density at point $\mathbf{r}$ for the whole integration area.

An improved correction, which partly takes edge effects of the system into account too, can be obtained by using the finite homogeneous sphere centered not at $\mathbf{r}_2 = \mathbf{0}$ but at $\mathbf{r}_2 = \mathbf{r}$, i.e., on the point where we are calculating the density of interaction energy,

$$\begin{aligned} u_0(\kappa, r) &= n_0 \frac{N-1}{2N} Q^2 \int_{\mathcal{S}(\mathbf{r},R)} d^3 r_2 n_0 \frac{e^{-\kappa|\mathbf{r}-\mathbf{r}_2|}}{|\mathbf{r}-\mathbf{r}_2|} \\ &= n_0^2 \frac{N-1}{N} Q^2 2\pi \int_0^R dr_2 r_2 e^{-\kappa r_2} \\ &= \frac{N-1}{N} Q^2 n_0^2 \frac{2\pi}{\kappa^2} [1 - e^{-\kappa R}(1+\kappa R)]. \end{aligned} \tag{A3}$$

This expression also has no divergent limit for $\kappa \to 0$, and, at the same time, yields monotonically decreasing density profiles as can also be seen in Fig. 3.

All these methods described above are compared, together with the MF approximation, in Fig. 8 showing the (effective) integration area of the methods. First consider the Coulomb case, i.e., that where the solid regions fill out the hatched ones and where the density is constant within the MF method too. There, the integration in Fig. 8(a) is equal to that in Fig. 8(c); thus the density obtained by the LDA (fs corrected) is equal to that of the MF method. In contrast to that, the effective integration area within Fig. 8(b) is infinite, leading to the breakdown mentioned above. In the case of finite screening, where effectively the integration area is reduced, Figs. 8(a) and 8(c) still have the same region of integration. But the constant approximation within Fig. 8(c), in contrast to Fig. 8(a), leads to an underestimation of the energy density in the outer region of the system—the high values of density toward the center will be ignored. Eventually this leads to the nonmonotonic density profile of the LDA (fs corrected). By contrast, Fig. 8(d) features an additional effective integration region, which partly prevents the underestimation, leading to the more accurate density profile of the LDA (partly fs corrected).

[1] D. J. Wineland, J. C. Bergquist, W. M. Itano, J. J. Bollinger, and C. H. Manney, Phys. Rev. Lett. **59**, 2935 (1987).
[2] M. Drewsen, C. Brodersen, L. Hornekaer, J. S. Hangst, and J. P. Schiffer, Phys. Rev. Lett. **81**, 2878 (1998).
[3] J. B. Pieper, J. Goree, and R. A. Quinn, Phys. Rev. E **54**, 5636 (1996).
[4] M. Zuzic, A. V. Ivlev, J. Goree, G. E. Morfill, H. M. Thomas, H. Rothermel, U. Konopka, R. Sütterlin, and D. D. Goldbeck, Phys. Rev. Lett. **85**, 4064 (2000).
[5] Y. Hayashi, Phys. Rev. Lett. **83**, 4764 (1999).
[6] Y. Ohashi, Phys. Rev. A **70**, 063613 (2004).
[7] C. J. Pethick and H. Smith, *Bose-Einstein Condensation in Dilute Gases* (Cambridge University Press, New York, 2002).
[8] A. Filinov, M. Bonitz, and Yu. Lozovik, Phys. Rev. Lett. **86**, 3851 (2001).
[9] H. Totsuji, C. Totsuji, T. Ogawa, and K. Tsuruta, Phys. Rev. E **71**, 045401(R) (2005).
[10] P. Ludwig, S. Kosse, and M. Bonitz, Phys. Rev. E **71**, 046403 (2005).
[11] M. Bonitz, D. Block, O. Arp, V. Golubnychiy, H. Baumgartner, P. Ludwig, A. Piel, and A. Filinov, Phys. Rev. Lett. **96**, 075001 (2006).
[12] V. Golubnychiy, H. Baumgartner, M. Bonitz, A. Filinov, and H. Fehske, J. Phys. A **39**, 4527 (2006).
[13] H. Baumgartner, H. Kählert, V. Golubnychiy, C. Henning, S. Käding, A. Melzer, and M. Bonitz, Contrib. Plasma Phys. **47**, 281 (2007).
[14] C. Henning, H. Baumgartner, A. Piel, P. Ludwig, V. Golubnichiy, M. Bonitz, and D. Block, Phys. Rev. E **74**, 056403 (2006).
[15] H. Totsuji, C. Totsuji, and K. Tsuruta, Phys. Rev. E **64**, 066402 (2001).
[16] H. Totsuji, J. Phys. A **39**, 4565 (2006).